

Fall 12-15-2022

## Fourier Acceleration in the Linear Sigma Model

Cameron Cianci  
cameron.cianci@uconn.edu

Follow this and additional works at: [https://opencommons.uconn.edu/srhonors\\_theses](https://opencommons.uconn.edu/srhonors_theses)



Part of the [Elementary Particles and Fields and String Theory Commons](#), and the [Quantum Physics Commons](#)

---

### Recommended Citation

Cianci, Cameron, "Fourier Acceleration in the Linear Sigma Model" (2022). *Honors Scholar Theses*. 926.  
[https://opencommons.uconn.edu/srhonors\\_theses/926](https://opencommons.uconn.edu/srhonors_theses/926)

# Fourier Acceleration in the Linear Sigma Model

Cameron Cianci

*University of Connecticut*

December 2022

**Honors Scholar Thesis**

*Department of Physics*

*Advisor: Dr. Luchang Jin*

*Honors Academic Advisor: Dr. Peter Schweitzer*

### Abstract

The linear sigma model is a low energy effective model of Quantum Chromodynamics. This model mimics the breaking of chiral symmetry both spontaneously and explicitly through the quark condensate and pion mass matrix respectively. Fourier acceleration is a method that can be implemented in the Hybrid Monte-Carlo algorithm which decreases autocorrelations due to critical slowing down through tuning the mass parameters in the HMC algorithm. Fourier acceleration is applied to the linear sigma model with a novel mass estimation procedure, by assuming the modes behave approximately like simple harmonic oscillators. The masses are chosen by sampling the expectation values of  $\langle \Pi \rangle$  and  $\langle |\phi_i(p) - \nu \delta_{i,0} \delta_{p,0}| \rangle$  (auxiliary momentum, and vacuum expectation of the fields) generated by the HMC algorithm. Additional findings in the linear sigma model during exploration of the symmetry breaking point are also discussed.

## 1 Introduction to the Linear Sigma Model

### 1.1 QCD and Effective Field Theories

Quantum Chromodynamics (QCD) is the currently accepted theory of the strong force [7]. QCD consists of Non-Abelian Gauge fields coupled to fermions with an  $SU(3)$  symmetry. Due to its strong coupling constant, perturbation theory cannot be used in low energy QCD, and instead the theory must be simulated on a lattice giving rise to the field of lattice QCD.

The full lattice QCD action can be resource and time intensive to simulate, and many effective theories such as chiral perturbation theory or the linear sigma model can be used as effective field theories to simulate low energy QCD at a lower computational cost. Effective field theories are field theories which incorporate the same symmetries as the high energy theory but integrate out high energy features,

absorbing the complexity of the high energy physics into the constants of the low energy effective theory. These effective theories are typically simpler than the full high energy theory and agree well with experimental results when restricted to low energies. When extending an effective theory to higher energies it is necessary to add many higher order terms, which greatly increases the complexity and cost of simulating the theory. Therefore effective field theories typically work well only when used as a low energy approximation to a more complex high energy theory.

Chiral symmetry is an important symmetry in QCD which the linear sigma model needs to mirror as a low energy effective theory. In QCD, neglecting the quark masses, the lagrangian of QCD is invariant under separate global transformations of the left-handed and right-handed quarks [10].

$$\mathcal{L}_{QCD} = -\frac{1}{4}Tr(G_{\mu\nu}G^{\mu\nu}) + i\bar{q}_L\gamma^\mu D_\mu q_L + i\bar{q}_R\gamma^\mu D_\mu q_R \quad (1)$$

When considering only the up and down quarks, this is invariant under a transformation of the type  $SU(2)_L \otimes SU(2)_R$ . This invariance is chiral symmetry, which the linear sigma model will need to replicate. However, this symmetry is broken both explicitly and spontaneously in QCD. This symmetry is explicitly broken by the quark mass terms. However, the up and down quarks are light, and therefore there is still an approximate chiral symmetry. This symmetry is also spontaneously broken by the quark condensate,  $\langle \bar{q}_{Rj}q_{Li} \rangle \neq 0$  [10]. We will need to mirror both of these aspects of chiral symmetry in the linear sigma model.

## 1.2 The Linear Sigma Model

The Lagrangian of the linear sigma model is [9],

$$\mathcal{L}_\sigma = \frac{1}{2}(\partial_\mu\sigma)^2 + \frac{1}{2}(\partial_\mu\boldsymbol{\pi})^2 - \frac{\mu^2}{2}(\sigma^2 + \boldsymbol{\pi}^2) - \frac{\lambda}{24}(\sigma^2 + \boldsymbol{\pi}^2)^2 - \bar{\psi}i\gamma^\mu\partial_\mu\psi + ig\bar{\psi}\boldsymbol{\tau}\gamma_5\psi + g\bar{\psi}\psi\sigma \quad (2)$$

Where  $\boldsymbol{\pi} = [\pi_0, \pi_+, \pi_-]$  are the pions,  $\sigma$  is the sigma particle, and  $\psi$  are the quarks. However, we will be restricting ourselves to the meson sector of this action,

$$\mathcal{L} = \frac{1}{2}(\partial_\mu\sigma)^2 + \frac{1}{2}(\partial_\mu\boldsymbol{\pi})^2 - \frac{\mu^2}{2}(\sigma^2 + \boldsymbol{\pi}^2) - \frac{\lambda}{24}(\sigma^2 + \boldsymbol{\pi}^2)^2 \quad (3)$$

This model is a scalar field theory with an  $O(4)$  symmetry between the  $\boldsymbol{\pi}$  and  $\sigma$  fields which is isomorphic to the  $SU(2)_L \otimes SU(2)_R$  chiral symmetry of QCD [9].

In addition to this, as there is both a negative mass-squared term  $-m^2\phi^2$  and an interaction term  $\lambda\phi^4$ , these terms together will result in spontaneous symmetry breaking. This spontaneous symmetry breaking mirrors the spontaneous breaking of chiral symmetry due to the quark condensate in QCD.

Spontaneous symmetry breaking occurs when the ground state energy of a system lacks an global symmetry of the system. Therefore when the system is forced into an unsymmetric ground state, it will spontaneously break the  $O(4)$  symmetry to an  $O(3)$  symmetry. As  $SU(2)$  is isomorphic to  $O(3)$ , this is equivalent to how the quark condensate spontaneously breaks the  $SU(2)_L \otimes SU(2)_R$  chiral symmetry to  $SU(2)_{L+R}$  [9]. This spontaneous symmetry breaking can be most easily understood by examining the 'mexican hat' potential (Figure 1) [1].

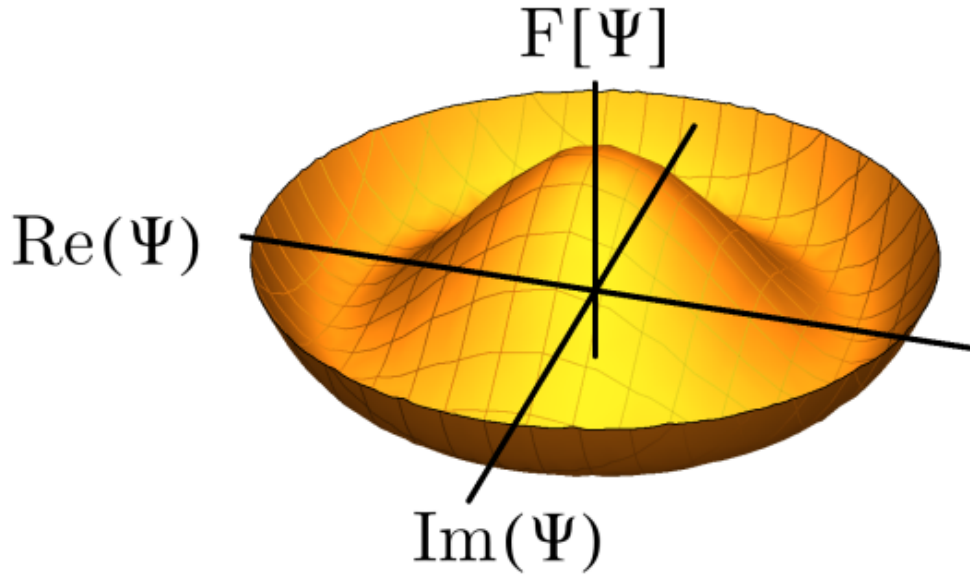


**Figure 1.** The 'Mexican-Hat' potential which illustrates spontaneous symmetry breaking in the linear sigma model. The linear sigma model has an  $O(4)$  symmetry, and therefore spontaneous symmetry breaking would occur in a 3-sphere rather than circularly as shown in this figure. Adapted from [1].

As can be seen above, the ground state of this system is not at the symmetric point  $\phi = 0$ , but instead, the  $\phi$  field gains a vacuum expectation value ( $\langle\phi\rangle = \nu$ ) which breaks the symmetry of the model.

In the linear sigma model, we define the  $\sigma$  field to be the field which gains a non-zero expectation value. The vacuum expectation value is determined by the potential  $V = -\frac{\mu^2}{2}(\sigma^2 + \boldsymbol{\pi}^2) - \frac{\lambda}{24}(\sigma^2 + \boldsymbol{\pi}^2)^2$ . Finding the minimum of this potential gives  $\langle\sigma\rangle = \nu = -(\frac{6\mu^2}{\lambda})^{1/2}$ . By redefining the  $\sigma$  field as  $\sigma' = \sigma + \nu$ , we can now rewrite the lagrangian of the theory after spontaneous symmetry breaking as,

$$\mathcal{L} = \frac{1}{2}(\partial_\mu\sigma)^2 + \frac{1}{2}(\partial_\mu\boldsymbol{\pi})^2 + \mu^2\sigma^2 - \frac{\lambda\nu}{6}\sigma(\sigma^2 + \boldsymbol{\pi}^2) - \frac{\lambda}{24}(\sigma^2 + \boldsymbol{\pi}^2)^2 \quad (4)$$

The most obvious difference is that the pions no longer have a quadratic term, and are therefore massless. This is due to the Goldstone theorem, which states that spontaneous symmetry breaking gives rise to massless Goldstone bosons [5]. Therefore the spontaneous breaking of this  $O(4)$  symmetry gives rise to 3 separate

Goldstone bosons, which are each of the pions ( $\boldsymbol{\pi} = [\pi_0, \pi_+, \pi_-]$ ). The pions still experience an  $O(3)$  symmetry after symmetry breaking.

However, the pions are not massless Goldstone bosons in QCD because of the quark mass matrix which explicitly breaks chiral symmetry. Due to this we need to explicitly break the linear sigma model's  $O(4)$  symmetry so that the Goldstone theorem does not hold and the pions can remain massive. This can be done by the addition of the explicit symmetry breaking term  $\mathcal{L}_b = \alpha\sigma$  to the meson sector lagrangian. The explicitly broken lagrangian is now,

$$\mathcal{L} = \frac{1}{2}(\partial_\mu\sigma)^2 + \frac{1}{2}(\partial_\mu\boldsymbol{\pi})^2 - \frac{\mu^2}{2}(\sigma^2 + \boldsymbol{\pi}^2) - \frac{\lambda}{24}(\sigma^2 + \boldsymbol{\pi}^2)^2 + \alpha\sigma \quad (5)$$

This new term also picks out a preferred direction for the vacuum state as well, incentivising the spontaneous symmetry breaking specifically along the  $\sigma$  direction. In addition, this term changes the vacuum expectation value to be approximately  $\nu = (\frac{6\mu^2}{\lambda})^{1/2} + \frac{\epsilon}{2\mu^2}$ , and gives the pions a mass of  $m_\pi^2 = \frac{\epsilon}{\nu}$ . It is worth noting that since the value of  $\epsilon$  is small, the  $O(4)$  symmetry is only slightly broken, and therefore the pions are 'approximate Goldstone Bosons', meaning that they will have a small mass. Eq. 5 defines the action of the linear sigma model explored in this paper.

## 2 Hybrid Monte-Carlo Algorithm

The Hybrid Monte-Carlo(HMC), also known as the Hamiltonian Monte-Carlo algorithm, is an algorithm used to create lattice configurations in lattice QCD. It was first proposed in [4] to simulate lattice QCD, but soon found utility in other scientific, medical, and industrial applications [2]. The HMC algorithm has found such utility because it is one of the most well proven and studied algorithms for determining expectation values in high dimensional statistical problems.

The HMC algorithm works to efficiently sample high dimensional statistical

data from a probability distribution specified by the partition function  $Z$ . The problem of high dimensional sampling of a probability distribution is difficult since as the dimensionality increases, there are many more unimportant directions where the probability distribution shrinks. This gives rise to the problem of creating an algorithm which best traverses a high dimensional probability distribution. It has been theoretically proven that the solution to the high dimensional sampling problem is to sample along the 'typical set' [2]. This therefore brings about the problem of how to stay within the typical set while still sampling from the entire probability distribution, and this is what the HMC algorithm solves.

The HMC algorithm works by expanding the target parameter space  $q$ , to include a new auxiliary momentum  $\pi(p, q)$ . The underlying physical connection between the target parameters and the auxiliary momentum ensures that by exploring the typical set of the auxiliary momentum, the algorithm will also explore the typical set of the desired probability distribution. However, now that the auxiliary momentum has been added we can use Hamilton's equations to evolve the target and auxiliary momentum parameters. As the Hamiltonian defines the energy of this fictitious system, comparing the starting and ending energies during a trajectory can show how closely the HMC algorithm is following the typical set. This value of energy gain/loss can then be used in a Metropolis-Hastings accept/reject step to help enforce that the HMC algorithm samples along the typical set rather than venturing outside of it.



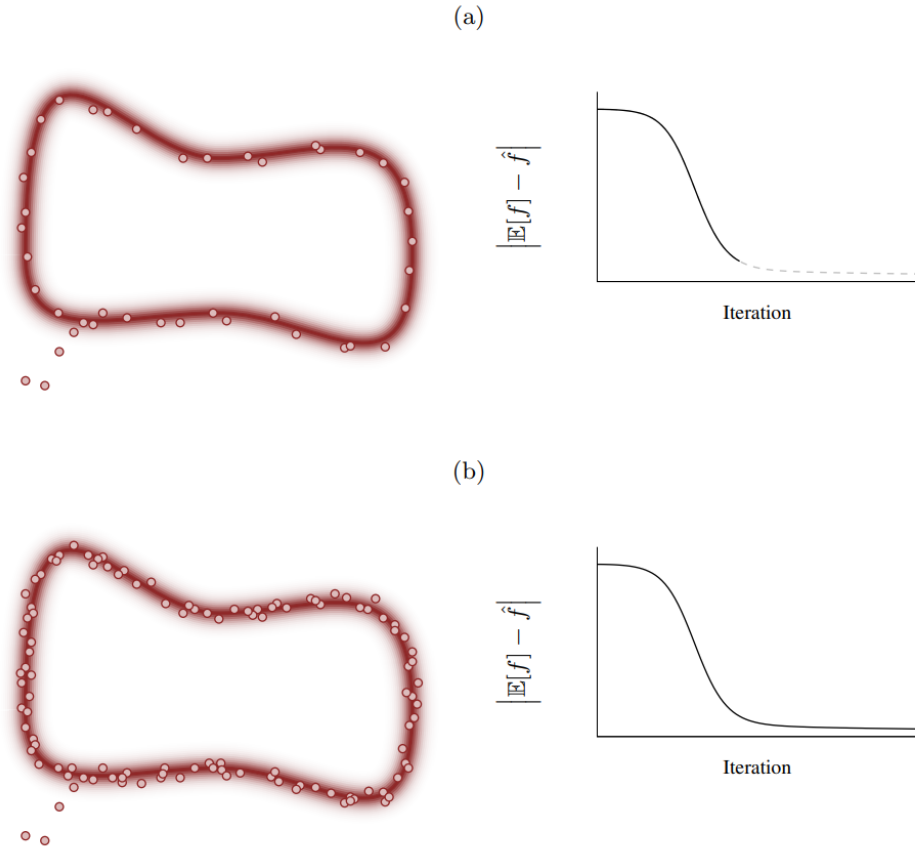


**Figure 2.** a) The HMC algorithm starts outside of the typical set, but quickly evolves to sample from within the typical set. b) The HMC algorithm converges to the correct expectation value after a sufficient time. Adapted from [2].

Lattice QCD also takes advantage of the connection between statistical mechanics and quantum field theory. Quantum field theory in Minkowski space has a metric  $[+, -, -, -]$ , such that the time component has a different sign than spatial components. However, after a Wick rotation to Euclidean time, the metric becomes  $[+, +, +, +]$ . This causes the time evolution operator to change from  $e^{-i\mathcal{H}t}$  to  $e^{-\mathcal{H}\tau}$ , changing the partition function from  $Z = \int D\phi e^{iS[\phi]}$  to  $Z = \int D\phi e^{-S_E[\phi]}$  [8]. The partition function in Euclidean time now appears like a statistical ensemble, and important quantities from quantum field theory such as the pion mass can be measured by sampling this statistical ensemble. This is the use of the HMC algorithm, to sample the statistical ensemble representing the Euclidean time field theory in order to obtain expectation values of relevant observables.

## 3 Fourier Acceleration

### 3.1 Critical Slowing Down

Critical slowing down occurs when lattice calculations are taken to the continuum limit. Extrapolating to the continuum limit requires calculations performed at increasingly small lattice spacing and therefore increasingly higher energies. Critical slowing down will occur due to the high energy modes which are added at smaller lattice spacing. These high energy modes require smaller step sizes to accurately integrate, while the low energy modes require larger step sizes.

In the HMC algorithm this leads to a problem, as the HMC algorithm treats all the modes equally and therefore every mode has an equal step size, and is limited by the high modes. This treatment leads to autocorrelations between adjacent lattice configurations generated by the HMC algorithm, as the low modes are not able to completely evolve to an uncorrelated value. The observables from the new trajectory will therefore be correlated with the previous trajectory. If these correlated configurations were directly used to determine observables, then the values of these observables would be likely incorrect and the errors of this calculation would be greatly underestimated. Due to this, many configurations must be generated before two uncorrelated lattice configurations can be sampled. This increases the amount of computational time required to perform lattice simulations, making it time and resource intensive to extrapolate to the continuum limit, which is the underlying reason for critical slowing down.

### 3.2 The Role of Fourier Acceleration

However, the HMC algorithm has one set of untouched but potentially tunable parameters, the masses in the kinetic term of the Hamiltonian. By tuning these masses, the low modes of the theory can be made to have smaller masses and the

high modes can be made to have larger masses. This results in a faster velocity (larger step size) for the low modes and a slower velocity (smaller step size) for the high modes. This approach is Fourier acceleration, and can allow for more efficient evolution of the high modes without reducing the global step size and therefore slowing the evolution of the low modes.

Fourier acceleration was first proposed in [6], where a 3-4x speedup was reported on an  $8^4$  lattice using the Jacobi algorithm to find efficient numerical solutions to the free Dirac equation, and then generalized this approach to the interacting case in QCD. This approach was later adapted to the HMC algorithm in a similar manner [3]. However, the first implementation was performed on a free theory, but QCD is a strongly coupled theory. Therefore, how is Fourier acceleration useful in a strongly coupled theory if it was designed to work for free field theories? The answer to this question is asymptotic freedom. QCD is an asymptotically free theory, meaning that the high energy modes couple more weakly than the low energy modes. This allows for the high energy modes to be approximately free and benefit from the smaller step size in Fourier acceleration, while the low modes still remain strongly coupled.

Essentially, in HMC without Fourier acceleration the high energy modes slow calculations by requiring smaller step sizes to be efficiently integrated. However, with Fourier acceleration these high energy modes are approximately free and no longer slow the HMC algorithm. Due to the application of Fourier acceleration, the HMC algorithm acquires a speed up on larger lattices with smaller lattice spacings, overcoming critical slowing down. There have been many promising results of Fourier acceleration in both scalar and gauge theories [3, 6, 11]. There are other important requirements when applying Fourier acceleration to gauge theories, as only certain gauge fixing terms allow for Fourier acceleration. However this research is performed on a strongly coupled scalar field theory, and does not have to deal with any of these complications.

## 4 Fourier Acceleration in the Linear Sigma Model

### 4.1 Choosing the Masses

The challenge of Fourier acceleration is how to tune the masses in order to optimally evolve each mode. Although the selection of masses is a solved problem for the free case, there may be more optimal ways to select the masses for the interacting case. The approach explored here assumed that the modes acted approximately like simple harmonic oscillators. Examining a classical simple harmonic oscillator, the equation of motion is simply,

$$m\ddot{x} = -kx \tag{6}$$

Which permits the solution,

$$x = A \cos(\omega t) \tag{7}$$

Applying two time derivatives to this solution demonstrates that  $\ddot{x} = -\omega^2 x$ . Since we want to set the masses such that the HMC algorithm evolves by  $\theta = \frac{\pi}{2}$  each timestep to be completely uncorrelated,  $\omega = \frac{\pi}{2}$ . Next, substituting this into  $F = m\ddot{x}$  therefore gives the solution,

$$m = -\frac{F}{\omega^2 x} = -\frac{4}{\pi^2} \frac{F}{x} \tag{8}$$

The next step is to generalize this classical formula to the HMC algorithm. In the HMC algorithm, the role of momentum is played by the auxiliary momentum parameters ( $\Pi$ ) and the role of position is the field values ( $\pi$  and  $\sigma$ ). Therefore,

when adapting this to the lattice we obtain,

$$m_i(p) = -\frac{4}{\pi^2} \frac{\langle |\dot{\Pi}_i(p)| \rangle}{\langle |\phi_i(p) - \nu \delta_{i,0} \delta_{p,0}| \rangle} \quad (9)$$

Where  $\phi_i = [\sigma, \pi_0, \pi_+, \pi_-]$ . The denominator in this expression is  $\langle |\phi_i(p) - \nu \delta_{i,0} \delta_{p,0}| \rangle$  instead of  $\langle \phi_i \rangle$  since the sigma field gains a vacuum expectation value which must be removed. Additionally, as  $\langle \dot{\Pi} \rangle$  and  $\langle |\phi_i(p) - \nu \delta_{i,0} \delta_{p,0}| \rangle$  are expectation values, we must run the HMC algorithm and sample these values over many lattice configurations before estimating the masses and beginning Fourier acceleration.

Since the assumption used is that the modes act approximately as simple harmonic oscillators, this approach is not likely to be very efficient for the strongly interacting low modes, but is likely to provide a speedup in the evolution of the weakly interacting high modes due to asymptotic freedom. Additionally, exploring this novel method for setting the masses in Fourier acceleration for the linear sigma model may give insights into implementing this mass estimation procedure in full QCD.

## 4.2 Experimental Results of Fourier Acceleration

Fourier acceleration was explored for many values of the parameters  $\alpha$ ,  $\lambda$ , and  $\mu^2$ . The quartic coupling constant  $\lambda$  was varied from  $2.5 \leq \lambda \leq 100000.0$ , and  $\mu^2$  and  $\alpha$  were varied accordingly in order to locate the physical values of  $F_\pi$  and  $m_\pi$ . Since we examined a large range of parameters, we can examine the performance of Fourier acceleration over both more weakly and strongly interacting cases.

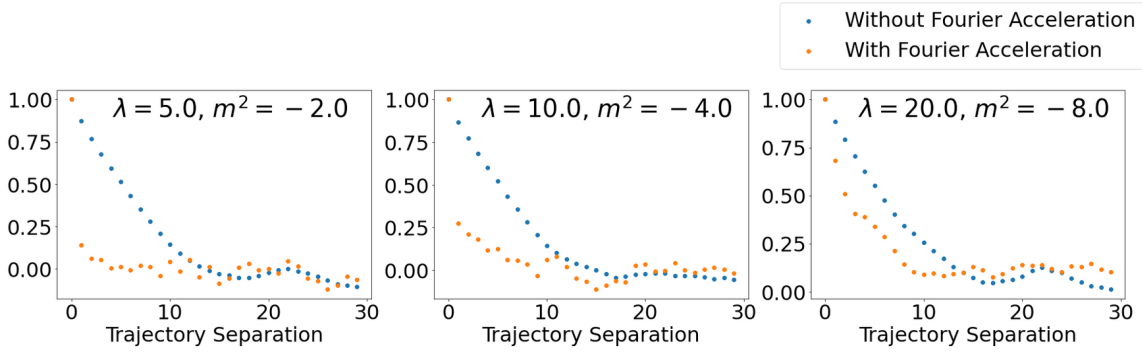


**Figure 3.** Autocorrelations of pion mass jackknife samples of an  $8^3 \times 16$  lattice,  $\alpha = 0.1$ .  $m_\pi \approx 0.3$  and  $F_\pi \approx 1.4 \pm 0.1$ . From left to right,  $m_\sigma \approx 1.0, 1.3$  and  $1.5$ .

As can be seen in Figure 3, Fourier acceleration with the novel mass estimation method greatly reduced autocorrelations for the  $\lambda = 5.0$  and  $10.0$  cases. The autocorrelations between adjacent configurations is reduced by approximately a factor of 5 in the  $\lambda = 5.0$  case, and approximately a factor of 2.5 in the  $\lambda = 10.0$  case. However, as the coupling  $\lambda$  increases, and the theory interacts more strongly. In these more strongly interacting cases, the assumption that modes behave like a simple harmonic oscillator begins to fail and the autocorrelations increase. This is demonstrated in the  $\lambda = 20.0$  case, where Fourier acceleration still decreases autocorrelation, but by significantly less than in the  $\lambda = 5.0$  and  $\lambda = 10.0$  cases.

This was performed on an  $8^3 \times 16$  lattice, which is a relatively small lattice by modern standards. As theorized by the original inventors of Fourier acceleration [6], Fourier acceleration's impact will increase on larger lattices due to the higher energy modes and asymptotic freedom. Therefore if more precise measurements on larger lattices are desired, this novel mass estimation method will likely only improve compared to this HMC baseline.

The lattices in Figure 3 had a lattice spacing of 70 MeV, therefore  $m_\pi = 21$  MeV, and  $m_\sigma = 70, 91,$  and  $105$  MeV respectively. As these pion and sigma mass values are unphysical, we also searched for other values of  $\alpha, \lambda,$  and  $\mu^2$  which could produce the physical values of  $F_\pi, m_\pi$  and an unstable  $\sigma$  particle. For a 1 GeV lattice this requires,  $F_\pi = 0.093, m_\pi = 0.135,$  and  $m_\sigma > 0.27$ . For a 500 MeV lattice  $F_\pi = 0.186, m_\pi = 0.27,$  and  $m_\sigma > 0.54$ .

During this search it was found that, although theoretically the  $\alpha$  parameter is thought to tune  $m_\pi$ , instead  $\alpha$  seemed to define the lattice spacing. This is likely due to the physical point being found near the symmetry breaking point, which allowed for  $\alpha$  to set the magnitude of both  $F_\pi$  and  $m_\pi$ . It was found that an  $8^3 \times 16$  1 GeV lattice required  $\alpha \approx 0.001$ , and a 500 MeV lattice required  $\alpha \approx 0.01$  for all explored values of  $\lambda$ . In addition, it was consistently found that  $\mu^2 \approx \frac{1}{5}\lambda$  produced the correct ratio between  $F_\pi$  and  $m_\pi$ .

### 4.3 The Symmetry Breaking Point

As the physical pion mass is small, the parameters explored were close to the symmetry breaking point. This allowed for observations to be made regarding spontaneous symmetry breaking in this model. As we desired the sigma to be unstable, we desired a way to determine whether the calculation was being performed in the symmetric or broken phase. While exploring the parameters, it was found that the effect of the alpha value on  $m_\pi$  and  $F_\pi$  was useful in determining the phase.

It is thought that the  $\alpha$  parameter in the linear sigma model should tune the pion mass in the broken phase. However, the symmetry breaking point does not seem to be well defined on a small lattice since the pion mass is so small, and  $\alpha$  affects both  $F_\pi$  and  $m_\pi$ . Therefore one common way to identify the symmetric from the broken phase was to measure the effect of tuning  $\alpha$  on the pion mass. The symmetry breaking point could be determined, as  $\alpha$  had a larger impact on  $m_\pi$  in the broken phase as shown on figures 4 and 5.

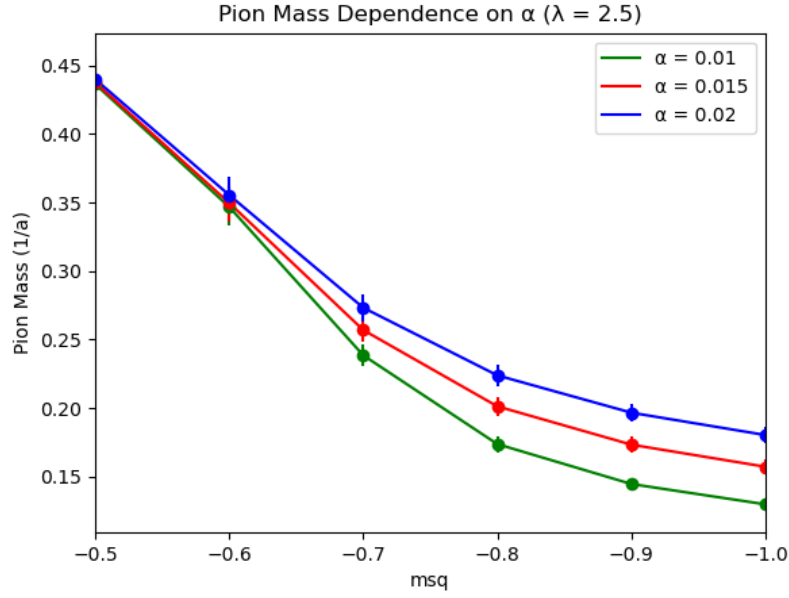


**Figure 4.** Pion mass dependence at varying  $\mu^2$  values. Changing the  $\alpha$  value has little effect at  $\mu^2 \leq -0.7$ , but has a greater effect at higher  $-\mu^2$ . As  $\alpha$  theoretically should tune the pion mass in the broken phase, the effect of  $\alpha$  on the pion mass could act as an indicator of the broken phase.

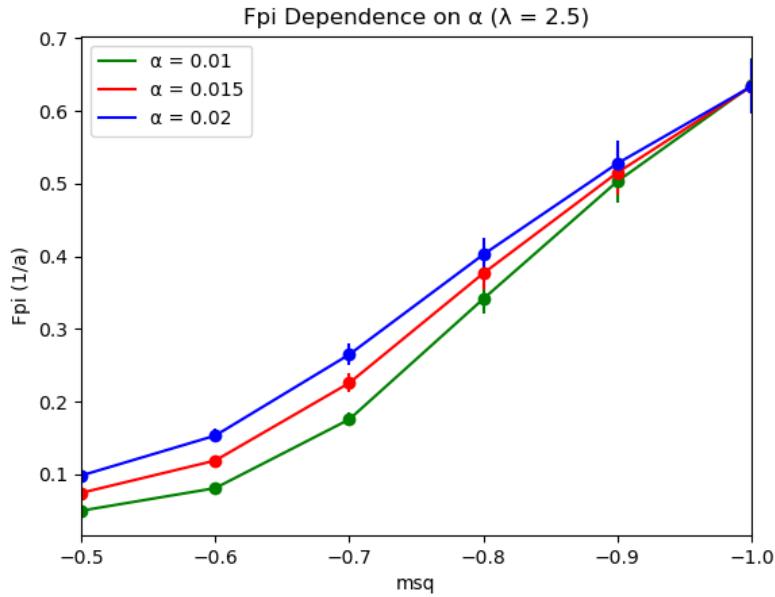


**Figure 5.**  $F_\pi$  dependence on  $\alpha$  for varying  $\mu^2$  values. It can be seen that  $F_\pi$  is affected oppositely of the pion mass. That is,  $F_\pi$  is less sensitive to the value of  $\alpha$  as  $\mu^2 \geq -0.7$ , and the theory enters the broken phase.



Since the pion mass is small, it was found that the physical parameters of the theory were close to the symmetry breaking point. As can be seen in Figures 4 and 5, the symmetry breaking point lies between  $-0.9 \leq \mu^2 \leq -0.6$ . As  $F_\pi$  is significantly affected by the value of  $\alpha$  in this region,  $\alpha$  mainly sets the magnitude of both  $F_\pi$  and  $m_\pi$ . This is likely the reason why  $\alpha \approx 0.001$  for all physical parameters in a 1 GeV lattice (Table 1). This affect of  $\alpha$  on the lattice may be due to the fact that a small  $8^3 \times 16$  lattice was used, as the symmetry is expected to break more sharply in larger lattices. Due to this, it is possible that in larger lattices  $\alpha$  will tune  $m_\pi$  significantly more than  $F_\pi$  and therefore act as expected.

During exploration of the parameter space, there was a difficulty in finding the physical parameters of the theory on a 1 GeV lattice due to the sigma mass, which was stable in almost all of the parameters explored. The sigma became more massive at higher  $\lambda$  values, and only became unstable at  $\lambda = 100000.0$  as is shown in Table 1. It is possible that, at larger lattice spacing and size, the  $\sigma$  particle may become even more massive as is shown in Table 2. This could suggest that finite volume effects may be playing a significant role on the  $8^3 \times 16$  1 GeV lattice.

$\lambda$	$\mu^2$	$\alpha$	$F_\pi$	$m_\pi$	$m_\sigma$
10	-2.825	0.0012	$0.0923 \pm 0.0018$	$0.1387 \pm 0.0016$	$0.1402 \pm 0.0031$
50	-12.5	0.001	$0.0886 \pm 0.0022$	$0.1314 \pm 0.0020$	$0.1368 \pm 0.0033$
5000	-1030	0.001	$0.0782 \pm 0.0018$	$0.1353 \pm 0.0020$	$0.1785 \pm 0.0049$
100000	-20550	0.0012	$0.0918 \pm 0.0044$	$0.1382 \pm 0.0042$	$0.2870 \pm 0.0218$

**Table 1.** Results for varying  $\lambda$ ,  $\mu^2$ , and  $\alpha$  with  $F_\pi$ ,  $m_\pi$  and  $m_\sigma$  near the physical values. Calculated with 2000 lattice configurations on a  $8^3 \times 16$  lattice. Notice that  $m_\sigma/m_\pi$  increases with increasing  $\lambda$  values. It is possible that the  $\sigma$  particle is unstable in the  $\lambda = 100000$  case, as  $m_\sigma/m_\pi > 2$ . However the errors are too large to definitively state this.

Lattice Size	$\lambda$	$\mu^2$	$\alpha$	$F_\pi$	$m_\pi$	$m_\sigma$
$8^3 \times 16$	10	-2.825	0.0012	$0.0923 \pm 0.0018$	$0.1387 \pm 0.0016$	$0.1402 \pm 0.0031$
$16^3 \times 32$	10	-2.78	0.001	$0.0823 \pm 0.0038$	$0.1322 \pm 0.0038$	$0.1556 \pm 0.0076$

**Table 2.** Results near the physical values for  $\lambda = 10.0$  for both a  $8^3 \times 16$  and  $16^3 \times 32$  lattice. Notice that  $m_\sigma/m_\pi$  is significantly larger in the  $16^3 \times 32$  lattice than the  $8^3 \times 16$  lattice.

## 5 Conclusion

A novel mass estimation procedure has been proposed and tested by approximating the modes of the HMC algorithm as simple harmonic oscillators, and sampling HMC trajectories to determine the masses of these oscillators. This procedure is expected to work well in weakly coupled modes, and experience worse performance in the more strongly coupled modes. Due to asymptotic freedom, this approach will likely still retain its utility for high momentum modes in a strongly coupled theory, and therefore work to overcome critical slowing down. Fourier acceleration with this novel mass estimation procedure has been demonstrated to reduce autocorrelations in the linear sigma model (Figure 3). However, the impact of this method decreases as the coupling constant increases.

In addition, the symmetry breaking point of the linear sigma model was investigated in an  $8^3 \times 16$  lattice. It was found that the symmetry breaking point could be defined by the effect of  $\alpha$  on  $f_\pi$  and  $m_\pi$ . The explicit symmetry breaking parameter  $\alpha$  has a greater impact on  $f_\pi$  in the symmetric phase, and a greater impact on  $m_\pi$  in the broken phase. An unstable  $\sigma$  particle was only found at  $\lambda \geq 100000$  for an  $8^3 \times 16$  lattice. It was found that increasing the lattice size to  $16^3 \times 32$  increased  $m_\sigma$ , and therefore it may be possible to find parameters with  $m_\sigma/m_\pi > 2$  at lower  $\lambda$  on a larger lattice. Lastly, it may be possible to adapt this novel mass estimation method in full QCD to address critical slowing down.

## References

- [1] Aron Beekman, Louk Rademaker, and Jasper van Wezel. An introduction to spontaneous symmetry breaking. *SciPost Physics Lecture Notes*, (0902.0885), dec 2019.
- [2] Michael Betancourt. A conceptual introduction to hamiltonian monte carlo. (arxiv:1701.02434), 2017.
- [3] Norman H. Christ and Evan W. Wickenden. Fourier acceleration, the hmc algorithm and renormalizability. (1812.05281), 2018.
- [4] Simon Duane, A.D. Kennedy, Brian J. Pendleton, and Duncan Roweth. Hybrid monte carlo. *Physics Letters B*, 195(2):216–222, 1987.
- [5] Jeffrey Goldstone, Abdus Salam, and Steven Weinberg. Broken symmetries. *Phys. Rev.*, 127:965–970, Aug 1962.
- [6] G. Katz, G. Batrouni, C. Davies, A. Kronfeld, P. Lepage, P. Rossi, B. Svetitsky, and K. Wilson. Fourier acceleration in lattice gauge theories. ii. matrix inversion and the quark propagator. *Phys. Rev. D*, 37:1589–1596, Mar 1988.
- [7] William J. Marciano and Heinz Pagels. Quantum Chromodynamics: A Review. *Phys. Rept.*, 36:137, 1978.
- [8] Michael E Peskin and Daniel V Schroeder. *An introduction to quantum field theory*. Westview, Boulder, CO, 1995. Includes exercises.
- [9] Nicholas Petropoulos. Linear sigma model at finite temperature. (hep-ph/0402136), 2004.
- [10] A. Pich. Introduction to chiral perturbation theory. *AIP Conf. Proc.*, 317(hep-ph/9308351):95–140, 1994. 46 pages, 4 figures (appended at the end), CERN-TH.6978/93.
- [11] Ahmed Sheta, Yidi Zhao, and Norman H. Christ. Gauge-fixed fourier acceleration. (2108.05486), 2021.